Semiconductor Physics, Quantum Electronics & Optoelectronics. 2003. V. 6, N 3. P. 282-286.

PACS: 61.46.+w; 61.72.Hh; 78.55-m; 78.66-w

Role of silicon oxide defects in emission process of Si-SiO_2 systems

M. Baran, B. Bulakh, N. Korsunska, L. Khomenkova, V. Yukhymchuk, M. Sheinkman
V. Lashkaryov Institute of Semiconductor Physics, NAS of Ukraine, 45 prospect Nauky, 03028 Kyiv, Ukraine
Phone: +38(044) 265 7234; fax: +38(044) 265 8342; e-mail: khomen@lumin.semicond.kiev.ua

Abstract. Si-rich SiO_2 films prepared by r.f. magnetron sputtering and annealed at 1150 °C are investigated by photoluminescence, Raman and EPR methods. It is found that emission spectrum of as-prepared samples contains one broad infrared band. It is shown that one-year aging in ambient air and low-temperature annealing in oxygen atmosphere lead to the increase of infrared band intensity and the appearance of additional bands with maxima at 1.7 eV, 2.06 eV and 2.3 eV while annealing in hydrogen atmosphere results in the decrease of 1.7 eV and 2.06 eV band intensities. The decrease of crystallite sizes results in high-energy shift of infrared band while the peak positions of another ones (at 1.7, 2.06 and 2.3 eV) do not change. It is concluded that infrared band is connected with Si crystallites while another ones can be ascribed to silicon oxide defects, 1.7 and 2.06 eV bands being ascribed to oxygen-excess defects such as EX- and non-bridging oxygen hole centres.

Keywords: photoluminescence; EPR; Si crystallites; EX-center; non-bridging oxygen hole centre.

Paper received 03.06.03; accepted for publication 17.06.03.

1. Introduction

In the last decade the great interest pays to the investigation of Si-SiO_2 systems due to their potential application for development of silicon-based light emitting devices. This is connected with the emission of such materials in wide spectral range at room temperature [1]. Electrochemical and chemical etching [1,2], laser ablation [3–5], ion implantation [6–8], thermal evaporation of SiO [9], magnetron sputtering [10–13] are used for production of Si-SiO_2 systems that can be considered as silicon crystallites embedded in oxide matrix. In some cases the following high temperature annealing is performed for creation of silicon crystallites. It is known that after such annealing Si-SiO_2 systems emit in red-orange spectral range. This emission is usually attributed to carrier recombination inside silicon crystallites [1,2] while alternative sources of red emission as surface states of Si nanocrystals [14], an exciton on Si/SiO_2 interface [15], electronic states at Si=O bonds [16] as well as oxide defects [17] are also proposed. However the nature of alternative radiative channels as well as their contribution to photoluminescence spectra are still under discussion and the clarification of these aspects are of great interest from fundamental viewpoint.

To elucidate the possible role of silicon oxide defects in emission process two approaches were used in this work. One of them is the changing of Si crystallites' sizes in wide range. It allows to separate the contribution of recombination inside Si crystallites from recombination through oxide defects due to different dependencies of peak positions of corresponding luminescence bands on crystallite sizes. The second approach is based on the possibility to vary the number of defects in silicon oxide during sample storage at the air (aging process) as well as under annealing in oxygen and hydrogen atmosphere.

2. Experimental procedure

Si-SiO_2 films were deposited on a long (15 cm) silicon or silicon oxide substrates by radio frequency magnetron sputtering from two (silicon and quartz) spaced-apart targets (Fig.1). This technique enables to vary the volume silicon content C_{Si} from 71 % down to 9 % along the length of the film (Fig. 1). C_{Si} was calculated as $C_{Si} = V_{Si}/(V_{Si} + V_{SiO2})$, where V_{Si}, V_{SiO2} are the volumes of Si and SiO_2. The films were annealed at 1150 °C in nitrogen atmosphere which leads to the formation of Si crystallites of varying sizes along the film. An additional

 © 2003, V. Lashkaryov Institute of Semiconductor Physics, National Academy of Sciences of Ukraine

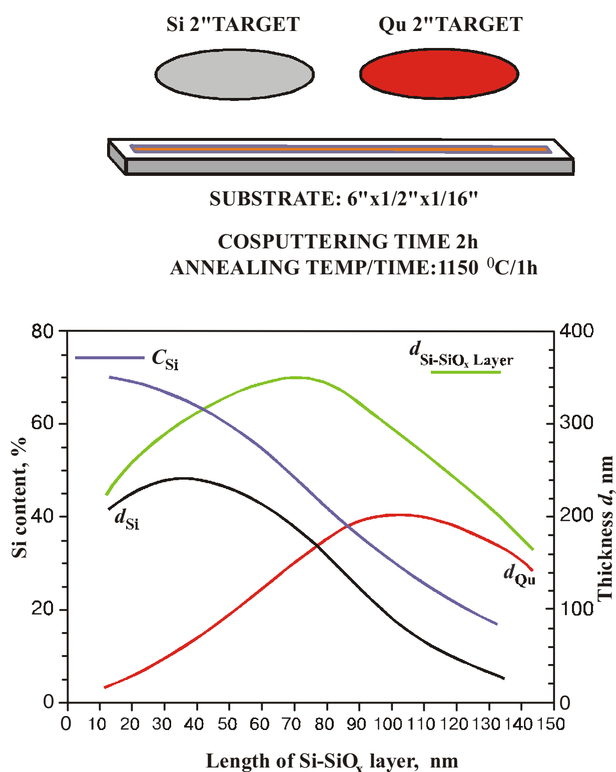

Fig. 1. Distribution of silicon content and thickness along Si-SiO_2 layer.

annealing in oxygen and hydrogen atmospheres at 160–360 °C was used to modify defect content. The variation of film characteristics during 1 year aging in ambient air was also studied.

The long substrates with the Si/SiO_2 layers were cut into parts of 0.5 cm length. PL was excited by an N_2 laser, dispersed with a prism spectrometer and registered by two photo multipliers (for different spectral ranges). The Raman spectra were measured as described in [10]. For EPR measurements a Varian-12 X-band spectrometer was used. All measurements were performed at room temperature.

3. Experimental results

3.1. As-prepared samples

PL spectra of as-prepared samples contain, as a rule, one broad infrared (IR) band (Fig. 2, curve 1). Its peak position shifts from 1.3 eV to 1.63 eV with the decrease of silicon content C_{Si} (Fig. 2, insert). The Raman scattering spectra demonstrate the presence of Si nanocrystals (Fig. 3). The peak position of the Raman signal at the Si-rich end (C_{Si} = 71–57 %) is 517 cm^{-1} (curves 1). With further C_{Si} decrease it shifts till 505 cm^{-1} (for C_{Si} ~ 30 %) and its full width at half maximum increases, corresponding to a change of sizes of Si nanocrystals from 5 nm to 2.7 nm (Fig. 3). It should be noted that the intensity of the Ra-

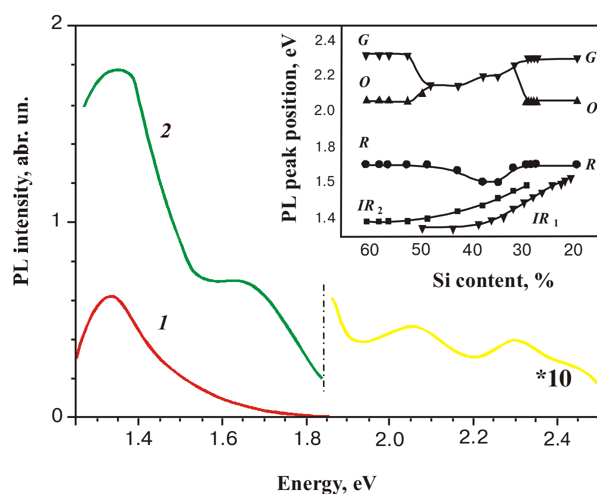

Fig. 2. PL spectra of as-prepared (*1*) and aged during one year at the air (*2*) Si-SiO_2 samples. C_{Si} = 52 %. Insert – Dependence of PL maxima positions of different bands on C_{Si} of as-prepared (IR_1) and one-year aged (IR_2, R,O,G) samples.

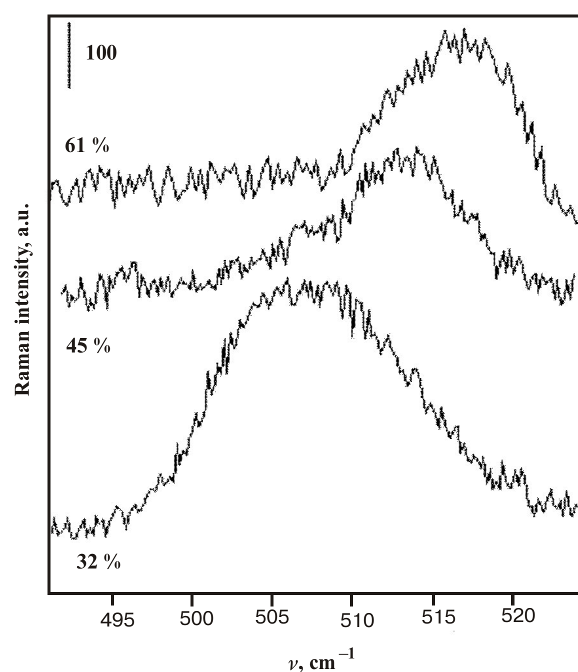

Fig. 3. Dependence of Raman spectra of Si-SiO$_x$ layer on C_{Si}.

man signal drops sharply when C_{Si} becomes less then 30 % and at the Si-poor end (C_{Si} = 30–20 %) it is not detected, implying a sharp decrease in the number of silicon nanocrystals. EPR spectra show the anisotropic signal with effective g = 2.0060 that can be assigned to silicon dangling bonds (possibly P_b-centers) (Fig. 4, curve 1).

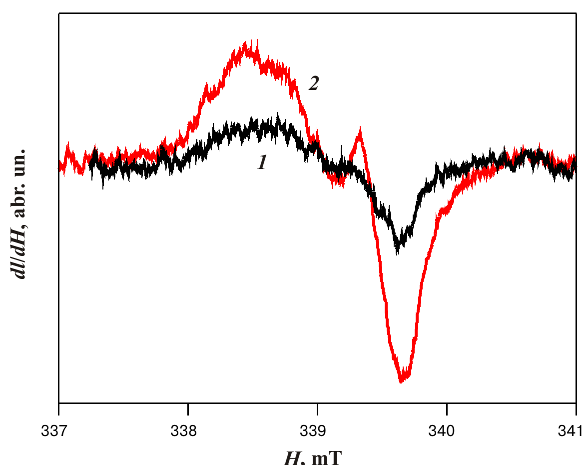

Fig. 4. EPR spectra of as-prepared (*1*) and aged during one year at the air (*2*) Si-SiO_2 samples. C_{Si} = 52 %.

3.2. Aged samples

One year aging in ambient air at room temperature leads to the increase of PL intensity and appearance of additional bands in red, orange and green spectral region (R-, O- and G-bands respectively) (Fig. 2, curve 2). The peak position of IR-band in aged sample is blue-shifted in comparison with peak position in as-prepared one (Fig. 2, insert). With silicon content decrease its maximum shifts to high-energy side as in the case of as-prepared samples. It should be noted that at Si-poor end IR-band is not detected.

At Si-rich end the peak positions of other bands do not change practically and are 1.7 eV (R-band), 2.06 eV (O-band) and 2.32 eV (G-band). At the Si-poor end peak positions of the R-, O- and G-bands are the same as at the Si-rich end of the sample (Fig. 1, insert).

At C_{Si} 57–33 % (intermediate region) the R-band shifts slightly to the low-energy side when the IR-band intensity increases and returns to its previous position when it decreases. Such behavior of the R-band can be explained by the overlapping of the R- and IR-bands at constant R-band peak position.

The maximum of O-band in the intermediate region of C_{Si} shifts up to 2.32 eV that corresponds to the G-band peak position (Fig. 2, insert). It should be noted that in this region the G-band is not observed separately. So, we can think that the gradual shift of the O-band from 2.06 eV to 2.32 eV is due to the superposition of O- and G-bands while the positions of the maxima of O- and G-bands do not depend on C_{Si}.

EPR spectrum of aged sample is shown on Fig. 4 (curve 2). After one year aging in addition to silicon dangling bond signal the isotropic signal with g = 2.0025 appears. This signal is connected with oxygen-excess defects such as EX-centers that contained four oxygen dangling bonds [23].

3.3. Annealing in different atmospheres

Additional annealing of as-prepared samples in oxygen atmospheres at 160–360 °C results in the increase of PL intensity, R-band intensity increasing mainly (Fig. 5, a). At the same time such treatment leads to appearance of EX-center signal (Fig. 5, b).

Annealing of aged samples in hydrogen at 360 °C leads to the increase of IR-band intensity while the intensities of other bands decrease, R-band intensity decreasing mainly (Fig. 6,a). At the same time silicon dangling bonds signal vanishes and intensity of EX-center signal decreases essentially (Fig. 6,b).

4. Discussion

As it follows from data described above, for all values of C_{Si} the peak positions of the three bands, R, O and G, do not shift with C_{Si}. At the same time IR-band shifts to high energy side with C_{Si} decreasing in the intermediate region. As one can see from Raman scattering spectra, the size of the Si nanocrystals decreases with C_{Si} decreasing in this region this correlates with the high-energy shift of

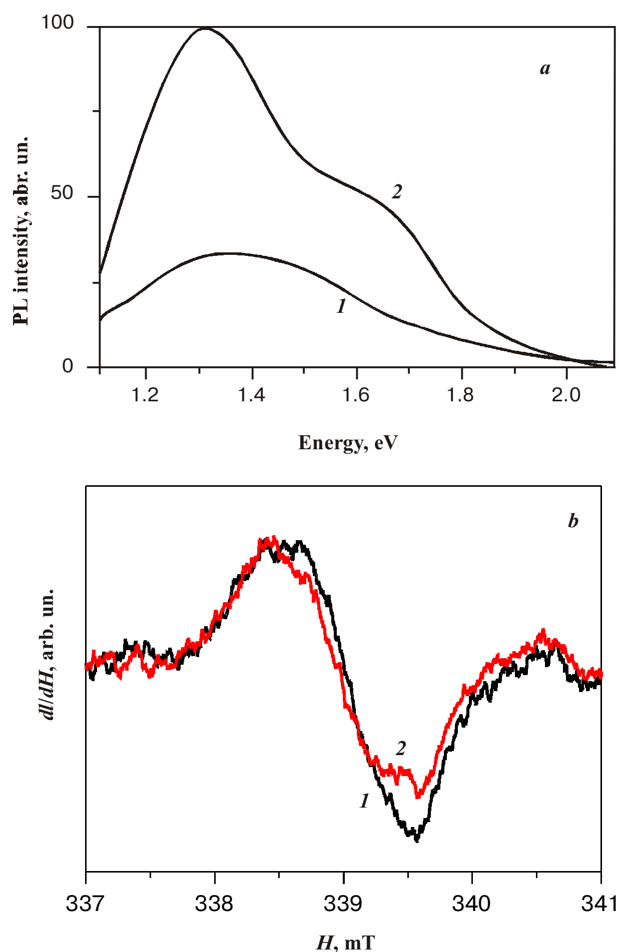

Fig. 5. PL (*a*) and EPR (*b*) spectra of as-prepared (*1*) and annealed at 180 °C in oxygen atmosphere samples.

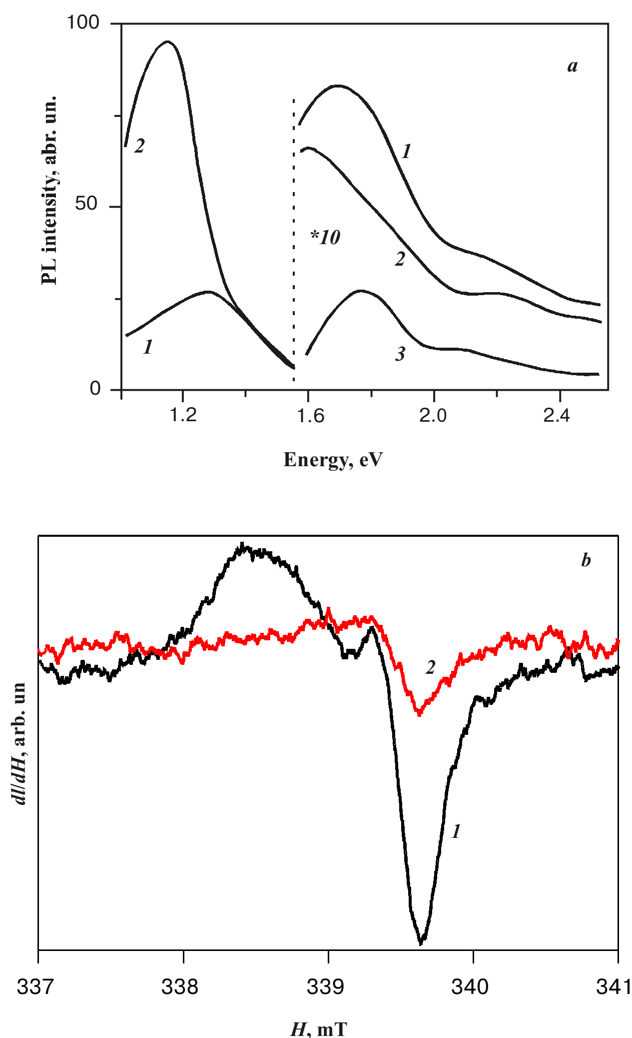

Fig. 6. PL (*a*) and EPR (*b*) spectra of one year aged (*1*) and annealed at 360 °C in hydrogen atmosphere samples. Curve *3* on Fig. 5a corresponds to difference of curve *2* and curve *1*.

IR-band. So, IR-band can be ascribed to exciton recombination in silicon nanocrystals and blue shift of its peak position during aging can be caused by a decrease of sizes of Si crystallites due to their oxidation.

Since the other bands keep their peak positions constant with C_{Si} changing we can conclude that these bands are due to carrier recombination through defect levels. Moreover this luminescence can be ascribed to intra-defect transitions. The following suggest that these defects are silicon oxide defects: i) the O- and G-bands were observed in silica optical fibers [18-20], silicate glass [11], in SiO_2 films implanted by different ions without following high-temperature annealing [7,9]; ii) R-, O- and G-bands appear during aging at the air that can be attributed to oxidation process.

G-band was ascribed to oxygen-deficient center, the O-band was attributed to non-bridging oxygen hole centers (NBOHC) [17,21,22] that is oxygen-excess defect while the nature of R-band is not clear up finally. This band was attributed to NBOHC (in non-oxidized porous silicon [17]) as well as to EX-centers (in porous silicon oxidized at high temperatures [21]). At the same time both centers are oxygen-excess defects and have to observed in oxidized samples.

It is known that EX-centers appear after high temperature annealing of silicon substrate in oxygen atmosphere. Our results show that these centers can appear during aging at room temperature also. Besides EX-center number increases under low temperature annealing of as-prepared samples at the air. In both cases the increase of EX-center number is accompanied by the increase of R-band intensity. So we can conclude that R-band is connected with EX centers.

The annealing in hydrogen atmosphere confirms this conclusion because it shows the simultaneous decrease of intensities of R-band and EPR signal from EX-centers. The latter is due to passivation of oxygen dangling bonds that are the part of EX-center.

It should be noted that since EX-center and NBOHC are oxygen-excess defects they are located in SiO_2, i.e. outside the interface area (SiO_x region).

Let us discussed the location of EX-centers in more detail. It is known that their number depends non-monotonically on oxide thickness [23]. The appearance of EX-centers have been observed when silicon oxide thickness reaches 4 nm. Then their number sharply increases up to 12.5 nm thickness. After this the decrease of EX-center number takes place. It have been supposed that this dependence is due to the reconstruction of silicon oxide structure with the increase of its thickness. Since these centers were not observed in thick oxide layers we can supposed that their appearance is connected with the presence of crystalline silicon. So, in spite of EX-centers are outlying from Si/SiO_2 interface we can conclude that these centers can follow up this interface, i.e. EX-centers appear interface centers.

As our results show the annealing of the samples in hydrogen atmosphere besides the decrease of EX-center number leads to the decrease of P_b-center one. It obviously is the reason of the increase of IR band intensity.

As for O-band, the decrease of its intensity under annealing in hydrogen can be explained by the passivation of oxygen dangling bonds that are the parts of these centers [22] as well as in the case of EX-centers.

5. Conclusions

It is found that PL spectrum of as-prepared $Si\text{-}SiO_2$ systems contains one broad infrared band. Its peak position shifts to high-energy side with the decrease of crystallite sizes results, that allows to ascribe it to exciton recombination inside silicon crystallites. One-year aging in ambient air leads to the increase of infrared band intensity

as well as the appearance of additional PL bands at 1.7 eV, 2.06 eV and 2.3 eV and EPR signal from EX-centers. The peak positions of the last three PL bands are independent on crystallite sizes. It is found that low-temperature annealing in oxygen atmosphere results in the main increase of 1.7-eV band intensity and simultaneous rise of EPR signal from EX-centers. Low-temperature annealing in hydrogen atmosphere leads to the opposite effect. Results obtained give the evidence that 1.7 eV, 2.06 eV and 2.3 eV bands are connected with silicon oxide defects. The first and second bands can be ascribed to EX-center and NBOHC that are oxygen-excess defects.

Acknowledgements

This work has been financially supported by National Academy of Sciences of Ukraine. One of the authors (L.Yu.K.) was supported by Grants of the President of Ukraine for young scientists.

References

1. *Light Emission from Silicon*, Eds. J.-C. Vial, L. T. Canham, W. Lang., North-Holland, Amsterdam, 1994.
2. V. Lehmann, U. Gosele, *Appl. Phys. Lett.*, **58**(10), p. 856 (1991).
3. A.V. Sachenko, E.B. Kaganovich, E.G. Manoilov, S.V. Svechnikov, *Semiconductors*, **35**(10), p. 1383 (2001).
4. A.V. Kabasin, M. Meunier, R. Leonelli // *J. Vac. Sci. Technol.*, B**19**, (2001) 2217.
5. L. Patrone, D. Nelson, V.I. Safarov, M. Sentis, W. Marine, S. Glorgio // *J. Appl. Phys.*, **87**, p. 3829 (2000).
6. T. Shimizu-Iwayama, N. Kurumado, D.E. Hole, P.D. Townsend // *J. Appl. Phys.*, **83**, p. 6018 (1998).
7. H.Z. Song, X.M. Bao // *Phys. Rev. B.* **55**, p. 6988 (1997).
8. B. Garrido, M. Lopez, S. Ferre, A. Romano-Rosrigez, A. Perez-Rodrigez, P. Ruterana, J.R. Morante // *Nucl. Instr. and Meth.*, **B120**, p. 101 (1996).
9. V. Ya. Bratus', V. A Yukhinchuk, L.I. Berezhinsky, M.Ya. Valakh, I.P. Vorona, I.Z. Indutnyy, T.T. Petrenko, P.E. Shepeliavyi, I.B. Yanchuk, *Semiconductors*, **35**(6), p. 763 (2001).
10. L. Khomenkova, N. Korsunska, T. Torchynska, V. Yukhymchuk, B. Jumayev, A. Many, Y. Goldstein, E. Savir, J. Jedrzejewski // *J.Phys.:Condens.Mater.*, **14**, p. 13217 (2002).
11. L. Khomenkova, N. Korsunska, V. Yukhimchuk , B. Jumayev, T. Torchynska, A. Many, E. Savir, Y. Goldstein, J. Jedrzejewski // *J.Lumin.*, **102-103**, p. 705 (2003).
12. K. Kohno, Y. Osaka, F. Toyomura, H. Katayama, *Jpn. J. Appl. Phys.* **33,** p. 6616 (1994).
13. Y. Kanzawa, T. Kageyama, S. Takeoka, M. Fujii, S. Hayashi, K. Yamamoto, *Solid State Commun.* // **102**, p. 533 (1997).
14. F. Koch, V. Petrova-Koch, T. Muschik // *J. Lumin.*, **57**, p. 271 (1993).
15. Y. Kanemitsu, Sh. Okamoto // *Phys. Rev. B.* **56**, p. R1696 (1997).
16. M.V. Wolkin, J. Jorne, P.M. Fauchet // *Phys. Rev. Lett*, **82**, p. 197 (1999).
17. S.M. Prokes, W.E. Carlos, O.J. Glembocki // *Phys. Rev. B.* **50**, p.17093 (1994).
18. L.N. Skuja, A.R. Silin // *Phys. Stat. Solidi A* **56**, p. K11 (1979).
19. K. Nagasawa, Y, Ohki, Y. Hama // *Jpn. J. Appl. Phys.*, **26**, p. L1009 (1987).
20. S. Munekuni, T. Yamanaka, Y. Shimogaichi, R. Tohmon, Y. Ohki, K. Nagasawa, Y. Hama // *J. Appl. Phys.*, **68**, p. 1212 (1990).
21. S.M. Prokes, W.E. Carlos // *J.Appl.Phys.*, **78**, p. 2671(1995).
22. T.V. Torchyska, N.E. Korsunska, L.Yu. Khomekova, S.M. Prokes // *Microelectronics Eng.*, **51-52**, p. 485 (2000).
23. A.Steasman // *J. Non-Cryts. Sol.*, **179**, p. 10 (1994).